Evolution in Electrical and Electronic Engineering Vol. 1 No. 1 (2020) 237 - 246

EEEE

Homepage: http://publisher.uthm.edu.my/proceeding/index.php/eeee
e-ISSN : 2756-8458

Remotely Control Wireless Movable Spotlight

Kho Wan Li[1], **Zuhairiah Zainal Abidin**[2]*

[1]Fakulti Kejuruteraan Elektrik & Elektronik,
Universiti Tun Hussein Onn Malaysia, Batu Pahat, 86400, Johor, MALAYSIA

[2]WARAS, Fakulti Kejuruteraan Elektrik & Elektronik,
Universiti Tun Hussein Onn Malaysia, Batu Pahat, 86400, Johor, MALAYSIA

DOI: https://doi.org/10.30880/eeee.2020.01.01.028
Received 15 August 2020; Accepted 06 September 2020; Available online 30 October 2020

Abstract: Remotely control wireless movable spotlight is one of a wireless power transfer that transmits power without connecting wires. Movable spotlight has some limitation in user design, which is the limited distance to adjust the movable spotlight position. This project was developed using near-field transmission concepts to solve distance limitation for the movable spotlight. A servo motor was used to improve the spotlight position at 0°, 90° and 180° angles. The servo motor was connected to a NodeMCU ESP8266 and controlled by Blynk app. Transmitter circuit consists of a transmitter coil and an oscillator circuit with a maximum working frequency of 180 kHz. Besides, the receiver circuit also has the receiver coil and a full bridge rectifier circuit. It shows that the remote control wireless movable spotlight is more convenient for users where it can be adjusted to the desired position using the Blynk app.

Keywords: Remotely Control, Near Field, Blynk App, NodeMCU ESP8266

1. Introduction

Wireless Power Transfer (WPT) transmits power without wiring. WPT comes from the electromagnetic induction principle. WPT is classified into two categories of wireless power transmission, such as near field and far field [1]. Power is transmitted by the magnetic field within a short distance using an inductive coupling concept for the wireless transfer of near field power. Moreover, power is transmitted by electromagnetic radiation beams, which can be transmitted over a long distance for wireless power transmission in far-field areas [2].

In the electromagnetic induction principle, it is the primary coil which generates the primary magnetic field, and the secondary coil is induced by the magnetic field [3]. The aspect of the electromagnetic spiral provides the circuit inductance. Inductance is an electrical feature of an electromagnetic belt opposite the current that flows through a circuit [4].

WPT will be used for the applications that require instantaneous energy and continuous energy delivery but due to conventional wires are high cost, inappropriate, dangerous and unnecessary [5]. In Wireless Power Transfer, the two main categories which are long range wireless power transfer and short range wireless power transfer. The main technique for long range wireless power transfer is

*Corresponding author: zuhairia@uthm.edu.my

realized by radio wave, laser or even ultrasound and short range wireless power transfer is inductive coupling [6]. The theory of wireless power transmission is suggested by Nicole Tesla [7]. Tesla continues to develop wireless distribution systems and he hopes that the system will be able to transfer power directly to homes and factories [8].

Movable spotlight has some limitation in the user design, which is the limited distance to adjust the position of the movable spotlight. This project will solve the problem of remote control of movable spotlight via wireless concepts. The main problem in this project is that the connection circuit comprises the coils that the electromagnetic induction occurs. Besides, the number of copper coils turns used must also be focused on which the amount of power transmitted can be determined.

2. Equipment and Methods

The circuit was categorized into two, the transmitter and receiver circuits. The transmitter circuit consists of an oscillator circuit and transmitter coil. And the receiver circuit consists of full bridge rectifier circuit and receiver coil. The voltage regulator is used to limit the DC voltage output to the device [9]. To control the spotlight at certain angles, the tower pro MG995 servo motor is used which controlled by a Blynk App via NodeMCU ESP8266 Wi-Fi module.

2.1 Equipment

Specifications and properties of materials and equipment used in the project are described in Table 1.

Table 1: Specifications and properties of equipments used in the project

Equipment	Function
NodeMCU ESP8266	Control the servo motor
Tower pro M995 servo motor	Control the position of spotlight
Oscilloscope	Indicate the input and output waveform of the circuits
Signal generator	Supply the signal to full bridge rectifier circuit
DC supply	Provide power source to the circuits
Resistors	Control the current flow
Capacitors	Smoothen the output of the circuits
Inductors	Store the energy
Diodes	Allow the current to flow in a direction
Voltage regulator	Maintain the output voltage to 5 V
Timer IC	Oscillate the pulse generation and voltage
Multimeter	Measure input & output of the voltage and current
Frequency counter	Measure the output frequency

2.2 Methods

Multisim software is used to design an oscillator and a full bridge rectifier. The servo motor and NodeMCU ESP8266 are used to control the position of the spotlight. The transmitter and receiver coils are then designed using ANSYS software. A simplified RLC circuit is then designed.

Figure 1 displays the oscillator circuit layout. To obtain the desired frequency, the TLC551CD timer IC is connected to and combined by various resistors and capacitors. The input of a timer IC is connected to a 12 V DC. By connecting to the oscilloscope, the waveform generated at the output is monitored. To obtain the induced output voltage, the multimeter is connected to the output of the oscillator circuit. Frequency counter is then connected to the output, and waveform frequency waveform are measured.

The circuit layout of the full bridge rectifier circuit is shown in Figure 2. The series of 1N4007 diodes with smoothing 1000 µF capacitors are used in this circuit. Diodes are connected to the AC input with 7 Vrms and 50 Hz input via function generator. Voltage regulator of LM7805CV is used to maintain the 5 V DC voltage on a full bridge rectifier circuit output. A 1000 µF capacitor is connected to the output of the voltage regulator to smooth the output DC voltage with a pure voltage. To observe the emitted waveform, an oscilloscope is connected to the output of full bridge rectifier. A multimeter is then connected to the full bridge rectifier circuit output to measure the output voltage.

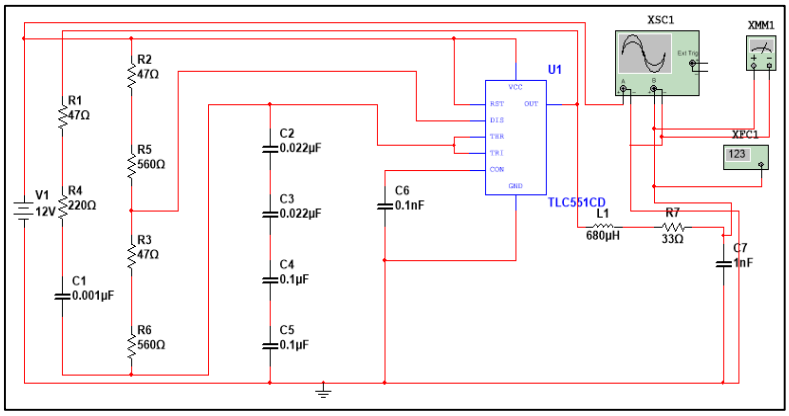

Figure 1: Oscillator circuit

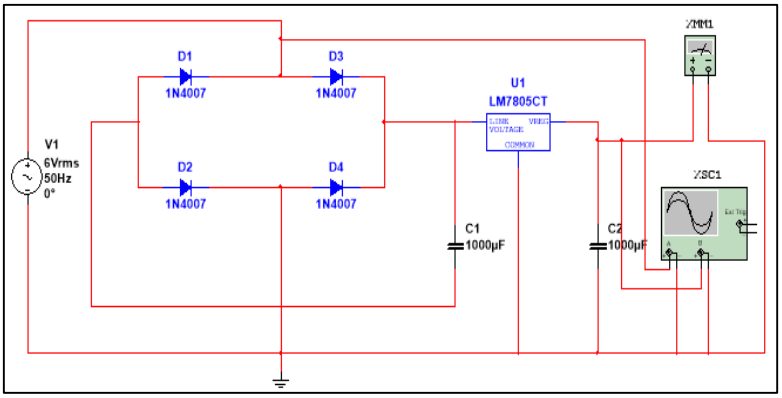

Figure 2: Full bridge rectifier circuit

The NodeMCU ESP8266 connection to the servo motor is shown in Figure 3. The Vin of NodeMCU ESP8266 is initially connected to the positive 6V DC adapter terminal. The ground is connected to the negative adapter terminal. The pulse width modulated (PWM) of the MG995 tower servo motor, which connects the wire in orange to digital output pin D2 of the NodeMCU ESP8266. The input and ground of the MG995 servo motor, which connects the red and brown wires to the positive and negative 6 V DC adapter terminal, respectively.

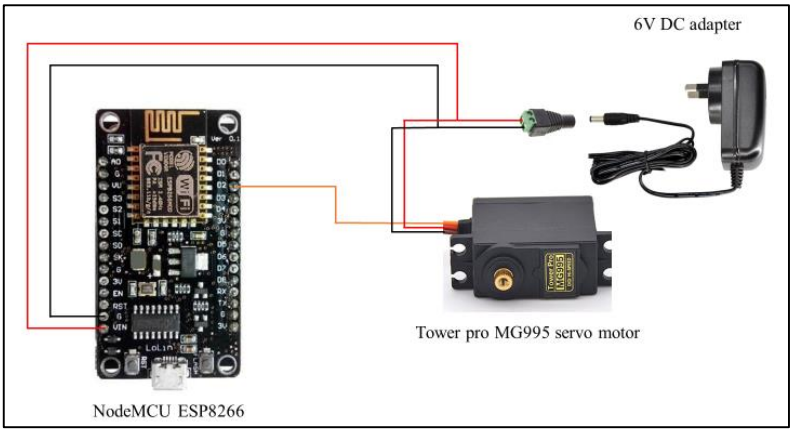

Figure 3: Connection of NodeMCU ESP8266 to tower pro MG995 servo motor

The programming flowchart of the servo motor is shown in Figure 4, to control the servo motor rotating at 0 °, 90 ° and 180 °. The Analog to Digital Converter (ADC) initially generates a digital value called the PotReading between 0 and 1023. The servo motor will turn from 0 ° to 180 ° when the Joystick is controlled, where the numeric value is mapped to ensure that the pulse width modulated digital output varies from 0 ° to 180 °.

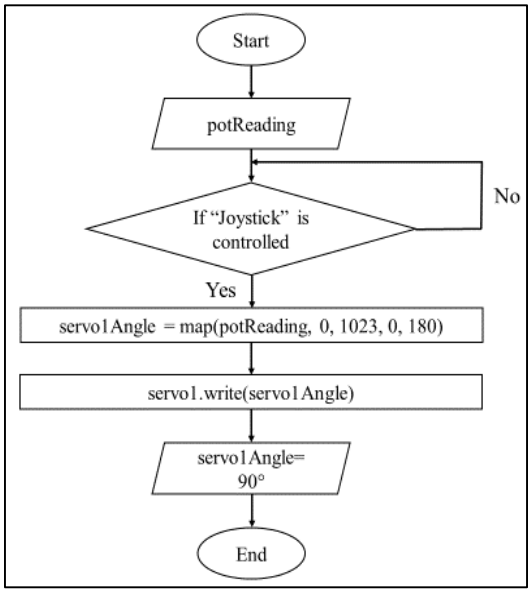

Figure 4: Programming flowchart of the servo motor

A "Joystick" and "Value Display" are used to control the pro-MG995 servo tower using the Blynk app. The "Joystick" function is to control the servo motor rotation by the user while the "value display" indicates the angle of rotation of the servo engine. The virtual pin V0 must be defined to "write" for the servo motor position, as shown in Figure 5. Meanwhile, a "Joystick" with output set from 0 to 1023 is used for servo position control. The virtual pin V1 is then used to read the motor position of the servo motor, as shown in Figure 5. A "Value Display" with the output defined from 0° to 180° is used in to show the servo motor positions.

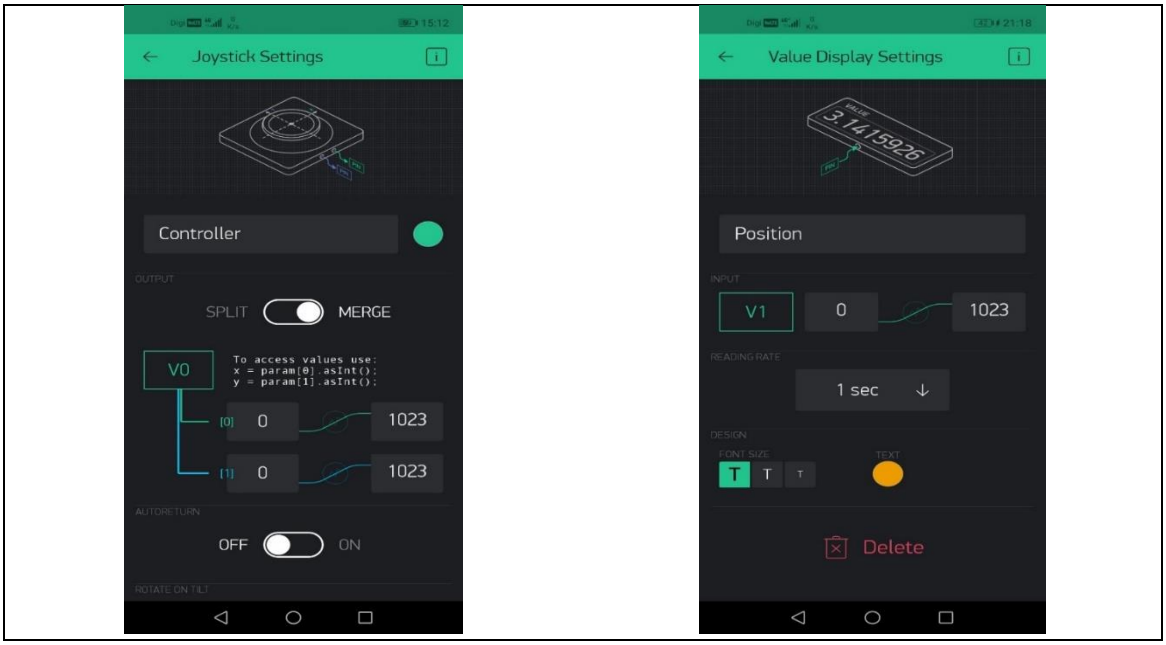

Figure 5: Setting of "joystick" and "value display" in blynk app

Figure 6 shows 20 cm distance between transmitter and receiver coils. The polygonHelix function was used to design transmitter and receiver coils, which can be found in ANSYS software's User Defined Primitive. The number of polygon cross-section segments was set to 0 as the copper coil used is round. After that, the outer radius of the cross-section polygon was set to 0.255 mm, the diameter of which is 0.51 mm. The transmitter and receiver coil radius was set to 30 mm, and the copper coil used was 5.6 m long. Based on Eq 1, copper coil turns used are 30 turns. The inductive coupling distance between the transmitter and receiver coils is within 20 cm based on Eq. 2.

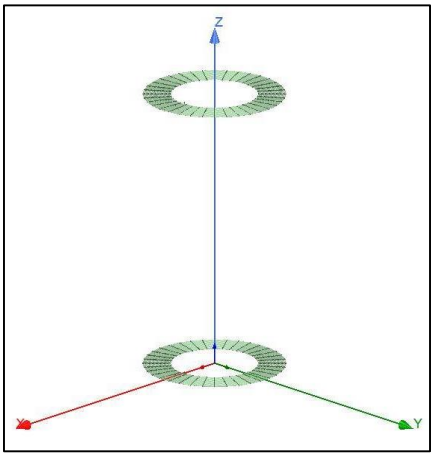

Figure 6: Transmitter and receiver coils separated by a distance of 20 cm

The simplified RLC circuit for wireless power transmission which is constructed using Proteus software is shown in Figure 7. The ammeter and voltmeter are connected to measure the output voltage and output current of the simplified RLC circuit. Besides, the voltage regulator is used to retain a 5 V output voltage. A DC motor is used where the speed of the motor can be calculated into angles using the equation in Eq. 3.

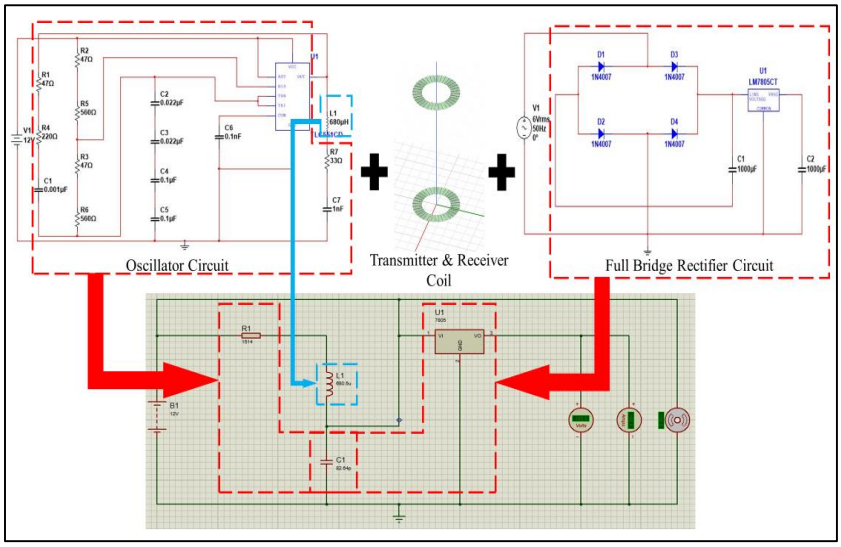

Figure 7: Simplified RLC circuit

The equations used are as the following:

$$\text{Number of turns of copper coil used, N} = \frac{L}{d} \qquad \text{Eq. 1}$$

where L is the length of copper coil used and d is the circumference.

$$\text{Reactive near field distance} \leq 0.62\sqrt{\frac{L^3}{\lambda}} \quad [10] \qquad \text{Eq. 2}$$

where L is the length of copper coil used and λ is the wavelength.

$$\text{X revolutions per minute} = \frac{\left(\frac{1}{60}\right)}{\left(\frac{1}{360}\right)} \times \text{X} = \text{Y degrees per second} \qquad \text{Eq. 3}$$

where X represents the value of RPM for DC motor and Y represents the value of degree per second after the RPM is converted [11].

3. Results and Discussion

The output waveform produced, output voltage and frequency of the oscillator and full bridge rectifier circuits can be obtained through Multisim software. The coupling coefficient, magnetic flux, impedance, resistance and inductance between the transmitter and receiver coils can be obtained in ANSYS software. Besides, magnetic field produced between transmitter coil and receiver coil also will be obtained in software. After that, the result of the simplified RLC circuit will also be obtained.

The input and output waveform produced by the oscillator circuit in Multisim software is shown in Figure 8. Besides, the output voltage and output frequency of oscillator circuit are 20.11 V and 185.667 kHz, respectively.

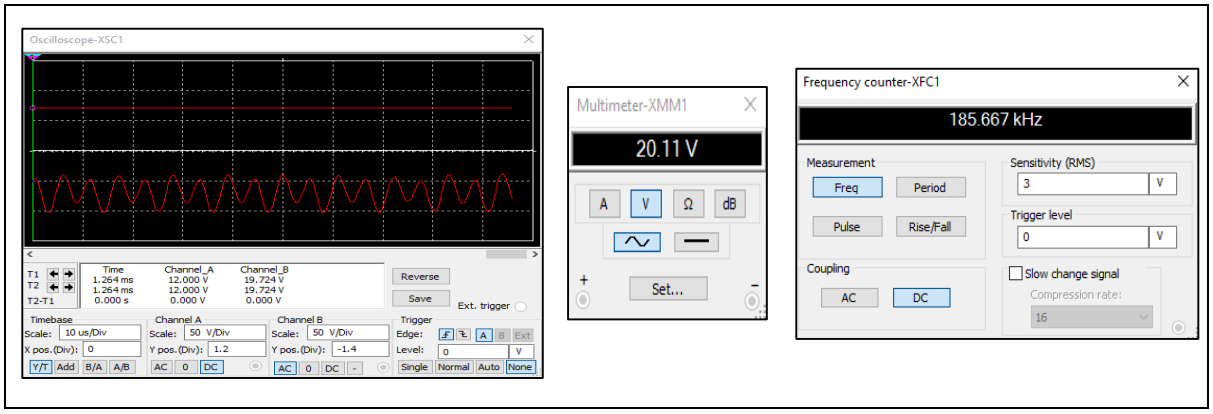

Figure 8: Output produced by oscillator circuit

Input and output waveform produced by the full bridge rectifier circuit in Multisim software is shown in Figure 9. The output voltage of the full bridge rectifier circuit is 4.973 V.

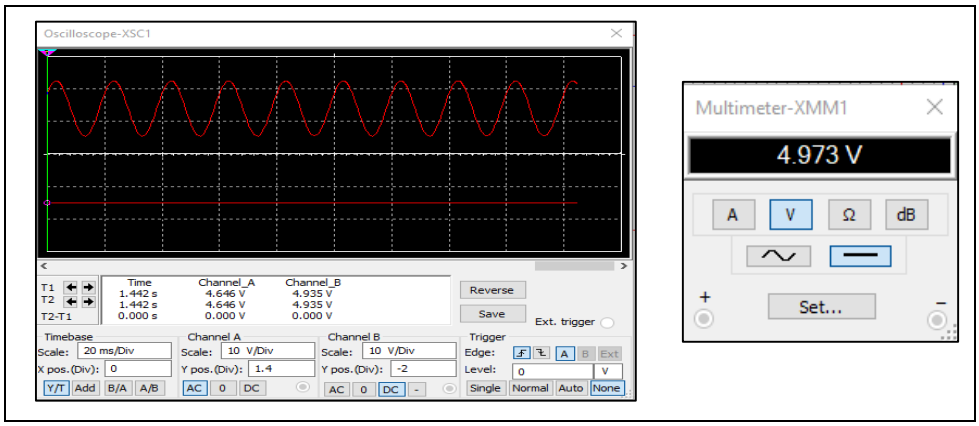

Figure 9: Output produced by full bridge rectifier circuit

The data obtained for the distance of 20 cm between the transmitter and receiver coils in software simulation is shown in Figure 10. Tx represents the transmitter coil and Rx represents the receiver coil. MagFlux is magnetic flux for the transmitter and receiver coils. For CplCoef, it is the coupling coefficient between the transmitter and receiver coils. Z represents the impedance, R represents the resistance and L is the self-inductance.

The coupling coefficient between the transmitter and receiver coils is the fraction of magnetic flux generated by the current in one coil which linked with another coil. Based on the distance among the transmitter coil and the receiver coil, only a portion of magnetic flux produced by transmitter coil will penetrate receiver coil and contribute to power transfer. Besides, magnetic flux generated by transmitter coil couples with the receiver coil. The magnetic flux density is depending on the distance separated between the transmitter and receiver coils.

As for the impedance, it is the effective resistance of a circuit to alternating current caused by the combined effect of ohmic resistance and reactance. The change in the impedance is caused by the shape of copper coil, size of copper coil, distance separation between the coil and the thickness of the material. Self-inductance refers to the changes in current in the circuit generate induced electromotive force in same circuit. The value of the inductance is depending on the number of turns of copper coil used and material of the core. When magnetic flux is strong, the value of the inductance will higher.

	1
Freq [kHz]	179.660000
Matrix1.MagFlux(Tx) [Wb]	0.000103 - 0.000001i
Matrix1.MagFlux(Rx) [Wb]	0.000001 - 0.000103i
Matrix1.Z(Tx,Rx) [ohm]	0.001269 + 0.565696i
Matrix1.R(Tx,Rx) [mOhm]	1.268973
Matrix1.L(Tx,Rx) [uH]	0.501132
Matrix1.CplCoef(Tx,Rx)	0.004888
Matrix1.L(Rx,Rx) [uH]	102.518166
Matrix1.L(Tx,Tx) [uH]	102.514834
Matrix1.R(Rx,Rx) [mOhm]	975.131414
Matrix1.R(Tx,Tx) [mOhm]	979.223527
Matrix1.Z(Rx,Rx) [ohm]	0.975131 + 115.726306i
Matrix1.Z(Tx,Tx) [ohm]	0.979224 + 115.722545i

Figure 10: Data obtained for transmitter and receiver coils

The magnetic field produced between the transmitter and receiver coils by the distance separation of 20 cm is shown in Figure 11. Inductive coupling take place between the transmitter and receiver coils which magnetic field produced. Based on the colour map in Figure 11, magnetic flux density produced is assessed. Therefore, in the concept of Biot-Savart's law, the nearer the distance separation between the transmitter coil and receiver coil, the stronger the strength of magnetic field and the magnetic flux density.

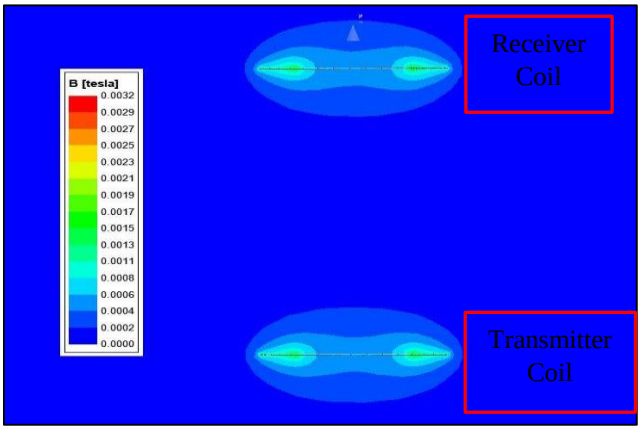

Figure 11: Magnetic field produced between transmitter and receiver coils

The output voltage and output current obtained in simplified RLC circuit are shown in Figure 12. The output voltage obtained is 5.01 V while the output current obtained is 1.00 A based on the simulation results. The mutual impedance is depending on the magnitude of the voltage induced and the phase difference between the voltage induced and the input current.

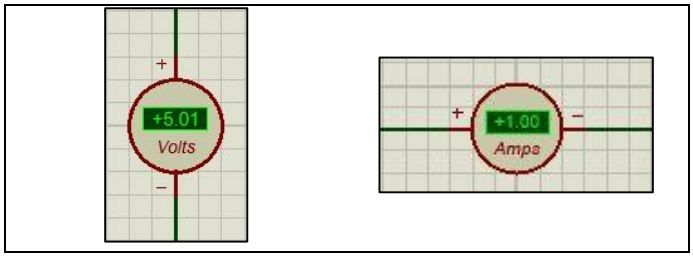

Figure 12: Output voltage and output current obtained in simplified RLC circuit

4. Conclusion

For the near-field wireless transmission, the transmitter and receiver circuits have been shown to play an essential role in this project. The physics behind the wireless power transmission used to design the transmitters and receivers are a crucial step in this project. The transmitter and the receiver circuits are designed with NI Multisim software, and the frequency of 185.67 kHz that is appropriate for the wireless power transmission near the field is observed. Besides, the transmitter and receiver coils are developed with ANSYS software. The magnetic field between the transmitter and the receiver is generated with a 20 cm radius. The transmitter and receiver coils were connected to the transmitter and receiver circuit, respectively. Besides, the servo motor has been rotated successfully at certain angles operated by the Blynk app. After the receiver circuit is connected to the servo motor, the wireless movable spotlight is successfully designed. The project objectives are, therefore achieved.

Some improvements are needed from this project to have a more functional system. During the design and investigations, the project recommendation is that more turns for transmitters and receivers be designed. The further transmitter and recipient coils are rotated, the higher the magnetic flux densities for inductive communication. Furthermore, with a higher number of turns, the distance between the transmitter coil and the receiver coil can be further increased. Also, the oscillator relaxation circuit can be substituted with the crystal oscillator circuit. That is because of the high-frequency reliability of the crystal oscillator circuit relative to the oscillative control circuit. However, regardless of variations in temperature and other parameters, the crystal oscillator has low-frequency drift.

Acknowledgement

The author would like to express deeply gratitude to UTHM and also thank to Faculty of Electrical and Electronic Engineering, Universiti Tun Hussein Onn Malaysia for the facilities.

References

[1] R. Shadid and S. Noghanian, “A Literature Survey on Wireless Power Transfer for Biomedical Devices,” Int. J. Antennas Propag., vol. 2018, 2018

[2] M. Etemadrezaei, “Wireless Power Transfer Seminar,” Power Electron. Handb., pp. 711–722, 2018

[3] W. P. Wamboka (2016) “Wireless Power Transmission” Final year project report, University of Nairobi, Kenya

[4] Anttijma (2015). Electromagnetic coils. Retrieved on October 10, 2019, from https://wiki.metropolia.fi/display/Physics/Electromagnetic coils

[5] Energypedia (2014). Wireless Power Transmission. Retrieved on October 23, 2019, from https://energypedia.info/wiki/Wireless_Power_Transmission

[6] Jamie MacFarlane (2018). Wireless Power Transfer. Retrieved on November 5, 2019, from http://large.stanford.edu/courses/2018/ph240/macfarlane2/

[7] M. M. El Rayes, G. Nagib, and W. G. Ali Abdelaal, “A Review on Wireless Power Transfer,” Int. J. Eng. Trends Technol., vol. 40, no. 5, pp. 272–280, 2016

[8] Wikipedia (2019). Wireless_power_transfer. Retrived on November 25, 2019, from https://en.wikipedia.org/wiki/Wireless_power_transfer

[9] T. Bartolotto, M. Tanwar, and Chuj (2018). Voltage Regulators. Retrieved on November 27, 2019, from https://www.circuitstoday.com/voltage-regulators

[10] Everything RF (2015). Antenna Near Field & Far Field Distance Calculator. Retrieved on April 6, 2020, from https://www.everythingrf.com/rf-calculators/antenna-near-field-distance-calculator

[11] Igor Gaspar (2020). Revolutions per minute to degrees per second conversion. Retrieved on May 10, 2020, from http://conversion.org/frequency/revolutions-per-minute/degrees-per-second